INNOVATIVE MECHANICAL ENGINEERING **ISSN 2812-9229 (Online)**
University of Niš, Faculty of Mechanical Engineering
VOL. 4, NO 2, 2025, PP 115-126

Original scientific paper*

NUMERICAL SIMULATION OF MHD NANOFLUID NATURAL CONVECTION HEAT TRANSFER IN A RECTANGULAR ENCLOSURE WITH DIFFERENT OBSTACLES

Ehsan Kianpour[1,2], Shiva Yadollahi[3]

[1] Department of Mechanical Engineering, Na.C., Islamic Azad University, Najafabad, Iran
[2] Aerospace and Energy Conversion Research Center, Na.C., Islamic Azad University, Najafabad, Iran
[3] Department of Industrial Engineering, Na.C., Islamic Azad University, Najafabad, Iran

Abstract. *This numerical study analyzes the cooling of different geometry hot obstacles within a rectangular cavity filled with water-CuO nanofluid under a magnetic field. The analysis assumes a two-dimensional, stable, laminar, and compressible flow. The cavity features an inlet and outlet, with the cold nanofluid entering from the left side and exiting from the opposite side after cooling the hot obstacle. All cavity walls are insulated and the SIMPLER algorithm is used to solve the governing equations. Various parameters, including nanoparticle volume fraction, Reynolds number, and Hartmann number, are examined. The results reveal that as the Reynolds number increases, the isothermal lines become more concentrated, and the cold zone near the inlet expands. This effect causes the isothermal lines to move closer to the hot obstacle, resulting in a steeper temperature gradient and enhanced heat transfer from the hot barrier.*

Key words: *Cooling, Nanofluid, Numerical simulation, Natural convection, Magnetic field*

1. INTRODUCTION

Conventional fluids typically have low thermal conductivity, which limits their heat transfer capabilities in industrial applications. To overcome this limitation and enhance heat transfer, nanofluids – dilute suspensions of nanoparticles in liquids, offer a promising

*Received: June 11, 2025 / Accepted August 08, 2025.
Corresponding author: Ehsan Kianpour
Faculty of Engineering, Najafabad branch, Islamic Azad University, Post code: 8514143131
E-mail: (ekianpour@pmc.iaun.ac.ir)

solution. Numerous studies have focused on developing empirical models for nanofluids, with the aim of applying these models to practical scenarios in nature and industry. Furthermore, the integration of nanofluids in cooling systems has emerged as a recent and highly active area of research, drawing significant attention from researchers [1-5]. Wang et al. [6] conducted a numerical study on the fluid flow and heat transfer of water-copper oxide nanofluid within a square cavity. The horizontal walls were insulated, while the left and right walls were maintained at hot and cold temperatures, respectively. Their findings indicated that when the effects of Brownian motion were considered, the average Nusselt number increased as the volume fraction of nanoparticles grew. Haddad et al. [7] also performed a numerical analysis to examine the impact of Brownian motion on natural convection heat transfer. They studied a water-copper oxide nanofluid in a chamber with cold upper and hot lower walls. Their results showed that heat transfer increased across all volume fractions, with the most significant enhancement occurring at lower volume fractions. Sharma et al. [8] investigated the forced convection heat transfer of a water-alumina nanofluid at low volume fractions in a heated channel. They found that the average Nusselt number increased with the nanoparticle volume fraction but decreased as the aspect ratio (defined as the width-to-height ratio) increased. Aghaei et al. [9] studied the velocity field and temperature distribution in a trapezoidal enclosure using the finite volume method. The working fluid was water with copper nanoparticles, leading to the consideration of a magnetic field within the enclosure. Their results showed that the nanoparticle volume fraction had a direct impact on increasing both the Nusselt number and entropy generation, whereas the Hartmann number exhibited the opposite effect. In a separate numerical study, Abbaszadeh et al. [10] employed the KKL model for a CuO-water nanofluid to account for the effects of Brownian motion of nanoparticles. They used the SIMPLER algorithm and the finite volume method to solve the Navier-Stokes equations (for flow field analysis) and the energy equation (for temperature distribution). In their study, Abbaszadeh et al. [10] considered a parallel plate microchannel geometry and applied the slip boundary condition on the walls. They incorporated the effects of the magnetic field through the Hartmann number. Their results indicated that increasing the fluid's inertia force, nanoparticle density, and the magnetic field effect led to higher total entropy production and an increase in the average Nusselt number. In a separate investigation, Ababaei et al. [11] utilized the finite volume method (FVM) to optimize the placement of obstacles within a microchannel to enhance the heat transfer rate. They worked with an Al2O3-water nanofluid, with the fluid properties modeled using the variable properties model proposed by Khanafer and Vafaei [12]. Their findings reinforced that increasing the momentum of the nanofluid boosts heat transfer inside the microchannel. They suggested that maintaining a sufficiently high Reynolds number is advantageous for augmenting the Nusselt number, although it also leads to an increase in total entropy generation. Recently, Hashim et al. [13] investigated the enhancement of heat transfer in an Al2O3-water nanofluid inside a wavy cavity using the finite element method. They applied partial heating to the bottom wall, while the wavy walls were kept isothermal, and the top wall was insulated. Different oscillation types for the wavy walls were tested to determine the optimal configuration for maximizing the Nusselt number. Their results demonstrated that the presence of nanoparticles enhanced the heat transfer rate within the cavity. A review of the existing literature reveals that the cooling of a hot, square-shaped obstacle within an enclosure has not been extensively studied. This study is

motivated by the need to quantitatively analyze the combined effects of magnetic fields, nanoparticle-enhanced fluids, and complex obstacle geometries on the enhancement and control of natural convection heat transfer within enclosures, addressing gaps in optimizing thermal performance in advanced cooling systems. Therefore, the primary objective of the present study is to numerically investigate the cooling of a hot barrier while considering the effects of the magnetic field within the enclosure. The walls of the enclosure are insulated, and the study examines the impact of fluid inertia, magnetic field strength, nanoparticle volume fraction, and outlet location on heat transfer. This analysis is conducted for Reynolds numbers ranging from 1 to 100, Hartmann numbers from 0 to 40, and nanoparticle volume fractions from 0% to 4%.

2. RESEARCH METHODOLOGY

The geometry of the enclosure is illustrated in Fig. 1. The cold nanofluid enters from the left side, flows through the cavity, and exits from the opposite side after cooling the hot obstacle. All walls of the enclosure are insulated, and the ratio of the length to width of the enclosure is 2. An aspect ratio of 2 is commonly used in studies related to natural convection in enclosures due to its ability to capture essential flow features, such as the development of secondary vortices, while maintaining a manageable computational domain. Several prior investigations have employed similar geometries in the context of nanofluid and MHD convection simulations [14,15].

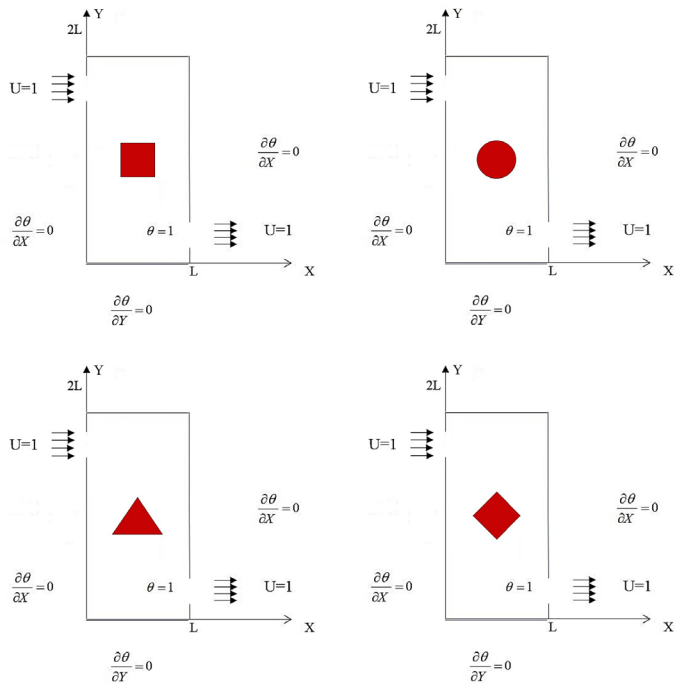

Fig. 1 Geometry and boundary conditions (dimensionless)

This choice provides a balance between physical representativeness and numerical stability. Additionally, the rectangular enclosure with this aspect ratio allows for a clear observation of boundary layer development along vertical and horizontal walls, which is crucial when evaluating heat transfer characteristics such as the Nusselt number. The hot obstacle has four different geometries, but all of them have the same cross-sectional area. The working nanofluid is an MHD CuO-water nanofluid, with its properties listed in Table 1.

Table 1 Thermo-physical properties of water as base fluid and CuO nanoparticles [16]

	ρ (kg/m3)	c_p (J/kgK)	k (W/mK)	d_{up} (nm)	σ $(\Omega m)^{-1}$
pure water	997.1	4179	0.613	--	0.05
CuO	6500	540	18	29	10^{-10}

The governing equations for laminar, natural convection flow of the nanofluid, including the Navier-Stokes equations and energy equation, are given as follows:

$$\frac{\partial}{\partial x}\left(\rho_{nf}u\right)+\frac{\partial}{\partial y}\left(\rho_{nf}v\right)=0 \tag{1}$$

$$\rho_{nf}\left(u\frac{\partial u}{\partial x}+v\frac{\partial u}{\partial y}\right)=-\frac{\partial p}{\partial x}+\mu_{nf}\left(\frac{\partial^2 u}{\partial x^2}+\frac{\partial^2 u}{\partial y^2}\right)-\sigma_{nf}B_0^2u \tag{2}$$

$$\rho_{nf}\left(u\frac{\partial v}{\partial x}+v\frac{\partial v}{\partial y}\right)=-\frac{\partial p}{\partial y}+\mu_{nf}\left(\frac{\partial^2 v}{\partial x^2}+\frac{\partial^2 v}{\partial y^2}\right)-\sigma_{nf}B_0^2v \tag{3}$$

$$\frac{\partial}{\partial x}\left(uT\right)+\frac{\partial}{\partial y}\left(vT\right)=\frac{\partial}{\partial x}\left(\alpha_{nf}\frac{\partial T}{\partial x}\right)+\frac{\partial}{\partial y}\left(\alpha_{nf}\frac{\partial T}{\partial y}\right) \tag{4}$$

In these equations, u and v represent the horizontal and vertical components of velocity, respectively, p is the pressure, T is the temperature, ρ_{nf} is the nanofluid density, $\nu_{nf}=\mu_{nf}/\rho_{nf}$ is the kinematic viscosity of the nanofluid, $\alpha_{nf}=\kappa_{nf}/(\rho c_p)_{nf}$ is the thermal diffusion coefficient of the nanofluid, and c_p is the heat capacity of the nanofluid at constant pressure. The dimensionless parameters used to cast the aforementioned equations into the non-dimensional form are as follows [17]:

$$\left(X,Y\right)=\frac{\left(x,y\right)}{L},\quad \left(U,V\right)=\left(u,v\right)\frac{L}{\alpha_{bf}},\quad P=\frac{pL^2}{\rho_{nf}\alpha_{bf}^2},\quad \theta=\frac{T-T_c}{\Delta T} \tag{5}$$

where $\Delta T=T_h-T_c$.

The continuity equation for the nanofluid flow expresses the conservation of mass and is generally the same as for conventional fluids, assuming the nanofluid behaves as a single-phase incompressible fluid. It ensures that the mass entering any control volume

equals the mass leaving it, implying no accumulation of mass. The continuity equation for 2D flow is expressed as below:

$$\frac{\partial U}{\partial x}+\frac{\partial V}{\partial y}=0 \tag{6}$$

$$\begin{aligned}&\frac{\partial}{\partial X}\left(UU\right)+\frac{\partial}{\partial Y}\left(VU\right)=\\&-\frac{\partial P}{\partial X}+\frac{\rho_{bf}}{\rho_{nf}\mu_{bf}}\frac{1}{\mathrm{Re}}\left[\frac{\partial}{\partial X}\left(\mu_{nf}\frac{\partial U}{\partial X}\right)+\frac{\partial}{\partial Y}\left(\mu_{nf}\frac{\partial U}{\partial Y}\right)\right]-\frac{\sigma_{nf}}{\sigma_{bf}}\frac{\rho_{bf}}{\rho_{nf}}\frac{Ha^2}{\mathrm{Re}}U\end{aligned} \tag{7}$$

$$\frac{\partial}{\partial X}\left(UV\right)+\frac{\partial}{\partial Y}\left(VV\right)=-\frac{\partial P}{\partial Y}+\frac{\rho_{bf}}{\rho_{nf}\mu_{bf}}\frac{1}{\mathrm{Re}}\left[\frac{\partial}{\partial X}\left(\mu_{nf}\frac{\partial V}{\partial X}\right)+\frac{\partial}{\partial Y}\left(\mu_{nf}\frac{\partial V}{\partial Y}\right)\right] \tag{8}$$

$$\frac{\partial}{\partial X}\left(U\theta\right)+\frac{\partial}{\partial Y}\left(V\theta\right)=\frac{\left(\rho c_p\right)_{bf}}{k_{bf}\left(\rho c_p\right)_{nf}}\times\frac{1}{\mathrm{Re}\,\mathrm{Pr}}\left[\frac{\partial}{\partial X}\left(k_{nf}\frac{\partial\theta}{\partial X}\right)+\frac{\partial}{\partial Y}\left(k_{nf}\frac{\partial\theta}{\partial Y}\right)\right] \tag{9}$$

The Reynolds, Hartmann, and Prandtl numbers are respectively defined as follows:

$$Re=\frac{u_0 L}{v_{bf}},\quad Ha=B_0 L\sqrt{\frac{\sigma_{bf}}{\mu_{bf}}},\quad Pr=\frac{v_{bf}}{\alpha_{bf}} \tag{10}$$

The properties of the nanofluid including density, heat capacity, volume expansion coefficient, diffusion coefficient are obtained as follows [18]:

$$\rho_{nf}=\left(1-\varphi\right)\rho_f+\varphi\rho_s \tag{11}$$

$$\left(\rho c_p\right)_{nf}=\left(1-\varphi\right)\left(\rho c_p\right)_f+\varphi\left(\rho c_p\right)_s \tag{12}$$

$$\left(\rho\beta\right)_{nf}=\left(1-\varphi\right)\left(\rho\beta\right)_f+\varphi\left(\rho\beta\right)_s \tag{13}$$

$$\alpha_{nf}=k_{nf}\Big/\left(\rho c_p\right)_{nf} \tag{14}$$

In the Maxwell-Brinkman model, the viscosity [13] and thermal conductivity coefficient [16], which depend solely on the volume fraction of nanoparticles, are determined using equations (15, 16).

$$\mu_{nf}=\mu_f\left(1-\varphi\right)^{-2.5} \tag{15}$$

$$k_{nf}=k_f\left(k_p+2k_f-2\phi\left(k_f-k_p\right)\right)\Big/\left(k_p+2k_f+\phi\left(k_f-k_p\right)\right) \tag{16}$$

For the water-copper oxide nanofluid, the λ and ζ corresponding functions are experimentally determined for the temperature range 300<T(K)<325 [3]:

$$\begin{aligned} \lambda &= 0.0137\left(100\varphi\right)^{-0.8229} \quad for \quad \varphi \le 1\% \\ \lambda &= 0.0011\left(100\varphi\right)^{-0.7272} \quad for \quad \varphi > 1\% \end{aligned} \tag{17}$$

The local Nusselt number is given by the following expression [19]:

$$Nu = \frac{q''(x).L}{k_{nf}.\left(T_w - T_\infty\right)} \tag{18}$$

Where $q''(x)$ is the local heat flux at the surface, L is the characteristic length, k_{nf} is the thermal conductivity of the nanofluid, T_w is the wall temperature and T_∞ is the ambient fluid temperature. The average Nusselt number can be calculated by inte

grating Eq. (18) along the surface of the hot obstacle:

$$Nu_{av} = \frac{\left(\int_L NudL\right)}{\left(\int_L dL\right)} \tag{19}$$

The Maxwell model equation estimates the effective electrical conductivity of the nanofluid by treating it as a two-phase mixture of the base fluid and dispersed nanoparticles. It accounts for the conductivities of both components and the volume fraction of nanoparticles suspended in the fluid. The model helps predict how adding conductive nanoparticles alters the overall electrical behavior of the fluid, which is important for applications involving electromagnetic fields or heat transfer.

$$\sigma_{nf} = \sigma_f \frac{\sigma_p + 2\sigma_f - 2\phi\left(\sigma_f - \sigma_p\right)}{\sigma_p + 2\sigma_f + \phi\left(\sigma_f - \sigma_p\right)} \tag{20}$$

where σ_{nf}, σ_f, σ_p and ϕ are the electrical conductivity of the nanofluid, the electrical conductivity of the base fluid, the electrical conductivity of the nanoparticles, and the volume fraction of the nanoparticles, respectively. The numerical method employed in this study is the SIMPLER algorithm combined with the Finite Volume Method (FVM). In this approach, a fine grid is initially defined over the problem domain, and a volume is assigned to each node. After integrating and discretizing the governing equations, the partial differential equations (PDEs) are simplified. The discretized equations are then solved using a line-by-line TDMA solver. To ensure the results are independent of the grid, the parameters of the average Nusselt number for grids with different dimensions are compared until changes in the grid dimensions no longer significantly affect these parameters (as shown in Table 2). Several simplifying assumptions are made in numerical modeling. These assumptions could contribute to slight discrepancies between simulated results and experimental data. It is important to note that such deviations are common in numerical simulations, especially when

simulating complex phenomena such as MHD nanofluid convection. While a 13.46% deviation is relatively large, it is within the typical range of variability found in similar studies involving nanofluids and MHD effects, as noted in previous works [14]. Also, the assumption of ideal dispersion for numerical modeling purposes means that the nanoparticles remain uniformly dispersed throughout the fluid without significant settling or clustering during the time scale of the heat transfer process. This assumption is commonly adopted in MHD nanofluid convection simulations [20].

Table 2 Average Nusselt number in *Ha*=40, *Re*=10 and ϕ=0.03

Grid size	Nu_{av}	Relative difference
41×21	19.14	--
81×41	16.10	13.46
161×81	16.38	1.74

3. RESULTS AND DISCUSSIONS

To validate the computer program used in this study, the results from Mahmoudi and Mazrouei [21] are modeled using the current numerical program, and their outcomes are compared and evaluated. The geometry of the setup used by Mahmoudi and Mazrouei [21] is shown in Fig. 2.

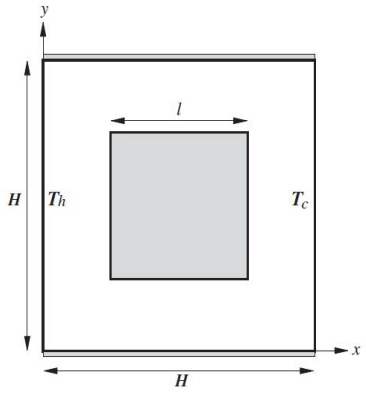

Fig. 2 The geometry of the Mahmoudi and Mazrouei [21]

In their study, they examined the problem of natural convection heat transfer of a copper-water nanofluid inside a square enclosure with a square insulating barrier placed at the center of the enclosure. As shown in Table 3, there is a good agreement between the results of the present study and the numerical results obtained by Mahmoudi and Mazrouei.

Fig. 3 demonstrates how the isothermal lines vary due to the presence of different obstacles at the Reynolds and Hartmann numbers of 100 and 40, respectively. Initially, the flow near the cold inlet interacts with the hot obstacle, gradually warming up the fluid.

As a result, the isothermal lines spread across the chamber, and a slight temperature gradient appears on the hot obstacle. When the Reynolds number increases, the isothermal lines become more compressed, causing the cold region near the inlet to expand.

Table 3 Comparison of average Nusselt number values on warm wall with Mahmoudi and Mazrouei research [21]

nanoparticle volume fraction	average Nusselt number values		difference percentage
	Mahmoudi and Mazrouei	Current study	
ϕ=0.0	9.6762	9.7918	1.2
ϕ=0.05	10.2635	10.4046	1.3
ϕ=0.10	10.8658	10.9789	1.0

This is due to the increased strength of the flow with the rising Reynolds number, which pushes the isothermal lines closer to the hot obstacle, resulting in a steeper temperature gradient and enhanced heat transfer from the hot obstacle. This effect is particularly noticeable with the diamond-shaped obstacle, where most of the chamber is filled with cold fluid, leading to more intense heat transfer on the hot obstacle. In contrast, for the square and triangular obstacles, the isothermal line pattern remains largely unchanged, with only minor adjustments attributed to the alterations in the flow pattern discussed earlier. Additionally, the temperature gradient on the hot obstacle is lower for the nanofluid compared to the base fluid, due to the thicker thermal boundary layer of the nanofluid, which arises from its higher thermal diffusivity.

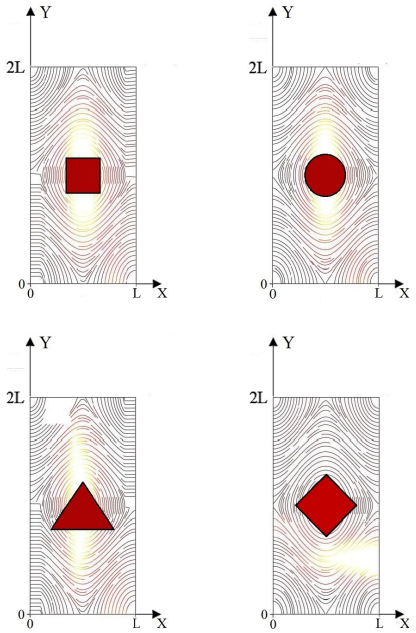

Fig. 3 Changes in streamlines with different obstacles for nanofluids at Reynolds and Hartmann numbers of 100 and 40

Fig. 4 illustrates the variation of the dimensionless temperature along the vertical axis at the central section of the enclosure for different Reynolds numbers, with Ha=20 and ϕ=4%. At Re=10, inertial forces are weak relative to viscous forces, resulting in asymmetric circulation where the right vortex dominates and the left one is weak. As the Reynolds number increases, inertia dominates, causing a reversal of vortex strength: the left circulation becomes larger and stronger while the right weakens. This leads to deeper hot-region penetration into the cavity core, enhanced nanoparticle mixing toward the walls, and overall increased convective heat transfer. Such behavior is consistently observed in MHD-driven nanofluid convection studies in rectangular enclosures, where increasing Re significantly enhances flow symmetry and heat transfer efficiency. When the Reynolds number increases from 1 to 100, the variation of the temperature remains largely unchanged due to the dominant influence of the magnetic forces (Ha=20). However, at Re=100, noticeable changes begin to appear, indicating a partial weakening of the magnetic suppression.

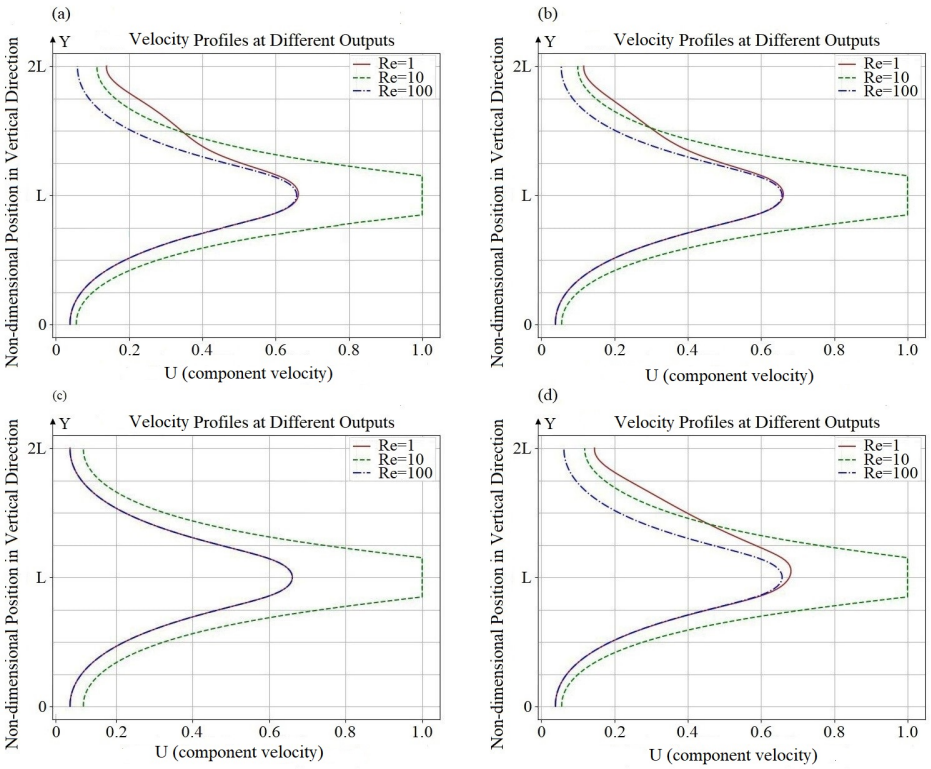

Fig. 4 Variations of the U component velocity with respect to the vertical location in the central section of the enclosure at different Reynolds numbers (Ha=20 and ϕ=4%): (a) rectangular obstacle, (b) circular obstacle, (c) triangular obstacle, (d) diamond obstacle

Fig. 5 presents the temperature distribution contours of the CuO nanofluid within a rectangular enclosure containing various obstacle shapes. In the absence of external forces, natural convection is driven solely by buoyancy effects resulting from temperature differences, which generate free convection currents that strongly impact the temperature field. The figure demonstrates that a circular obstacle induces symmetrical flow separation, allowing temperature contours to smoothly diverge around its surface. In contrast, a square obstacle introduces sharp edges that lead to flow detachment and the formation of recirculation zones, with thermal boundary layers developing along its flat faces. For the triangular obstacle, concentrated thermal regions are observed near the corners due to localized flow disruptions and sharper temperature gradients.

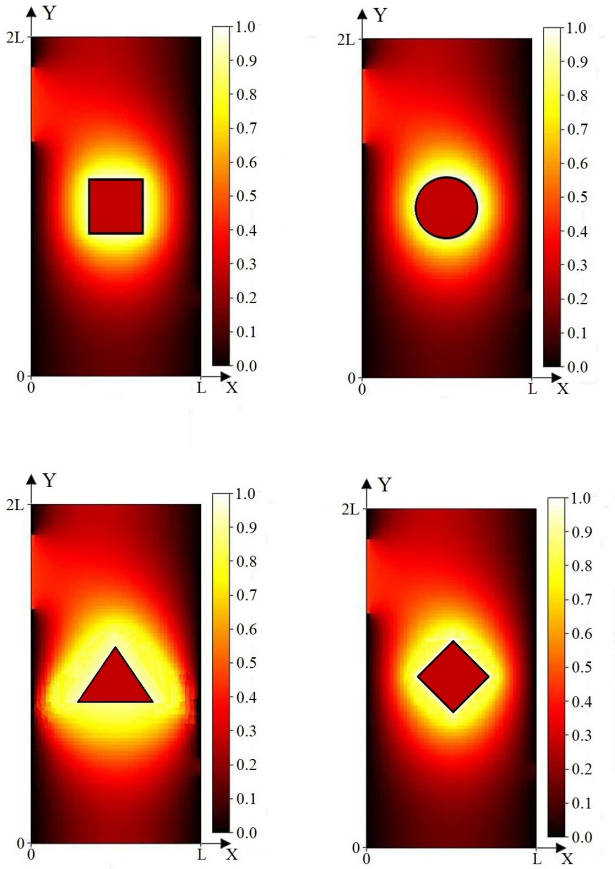

Fig. 5 Temperature distribution contours for different obstacles with CuO nanofluid at Re=100, Ha=20 and ϕ=4%

4. CONLUSIONS

This study comprehensively examined the heat transfer characteristics of an MHD CuO-water nanofluid flowing through an enclosure containing hot obstacles in the middle of a rectangular cavity with varying geometries but equal cross-sectional areas. Utilizing the SIMPLER algorithm coupled with the Finite Volume Method ensured accurate numerical modeling validated against previous work, confirming the reliability of the results. The cavity had an inlet and an outlet, walls were insulated, the barrier in the middle of the cavity was warm, and the effects of fluid inertia, magnetic field strength, volume fraction of nanoparticles on the heat transfer rate were investigated. The simulation was performed for Re=1- 100, Ha=20, and ϕ=4%. The results showed that:

1- The diamond-shaped obstacle notably enhanced heat transfer by promoting a wider cold fluid region near the inlet and intensifying temperature gradients on the obstacle surface.
2- The magnetic field and Reynolds number interplay demonstrated that stronger flows could partially counteract magnetic suppression effects, altering velocity profiles and thermal boundary layers.
3- The nanofluid's higher thermal diffusivity resulted in thicker thermal boundary layers and consequently lower temperature gradients on the heated surfaces compared to the base fluid.
4- These findings underscored the critical role of obstacle geometry and flow parameters in optimizing heat transfer in MHD nanofluid systems, providing valuable insights for designing efficient thermal management devices.

REFERENCES

1. Al-Farhany, K., Abdulkadhim, A., Hamzah, H.K., Ali, F.H., Chamkha, A., 2022, MHD effects on natural convection in a U-shaped enclosure filled with nanofluid-saturated porous media with two baffles, Progress in Nuclear Energy, 145, pp. 104136.
2. Alsabery, A.I., Abosinnee, A.S., Al-Hadraawy, S.K., Ismael, M.A., Fteiti, M.A., Hashim, I., Sheremet, M., Ghalambaz, M., Chamkha, A.J., 2023, Convection heat transfer in enclosures with inner bodies: A review on single and two-phase nanofluid models, Renewable and Sustainable Energy Reviews, 183, pp. 113424.
3. Kianpour, E., Dehkordi, S.M.H.R., Sidik, N.A.C., 2024, Numerical Simulation of MHD Nanofluid Forced Convection Heat Transfer in a Rectangular Enclosure with Variable Parametersters. Innovative Mechanical Engineering, 3(2), pp. 43-55.
4. Mebarek-Oudina, F., Chabani, I., 2022, Review on Nano-Fluids Applications and Heat Transfer Enhancement Techniques in Different Enclosures, Journal of Nanofluids, 11(2), pp. 155-168.
5. Rostami, S., Aghakhani, S., Hajatzadeh Pordanjani, A., Afrand, M., Cheraghian, G., Oztop, H.F., Safdari Shadloo, M., 2020, A review on the control parameters of natural convection in different shaped cavities with and without nanofluid, Processes, 8(9), pp. 1011.
6. Tongsheng, W., Li, A., Xi, G., Huang, Z. 2023, Conjugate MHD natural convection of hybrid nanofluids in a square enclosure containing a complex conductive cylinder, International Journal of Numerical Methods for Heat & Fluid Flow, 33(3), pp. 941-964.

7. Haddad, Z., Iachachene, F., Abu-Nada, E., Pop, I., 2020, Investigation of the novelty of latent functionally thermal fluids as alternative to nanofluids in natural convective flows, Scientific Reports, 10(1), pp. 20257.
8. Sharma, M., Sharma, B.K., Kumawat, C., Jalan, A.K., Radwan, N., 2024, Computational Analysis of MHD Nanofluid Flow Across a Heated Square Cylinder with Heat Transfer and Entropy Generation, Acta Mechanica et Automatica, 18(3), pp. 536-547.
9. Aghaei, A., Khorasanizadeh, H., Sheikhzadeh, G., Abbaszadeh, M., 2016, Numerical study of magnetic field on mixed convection and entropy generation of nanofluid in a trapezoidal enclosure, Journal of Magnetism and Magnetic Materials, 403, pp. 133-145.
10. Abbaszadeh, M., Ababaei, A., Abbasian Arani, A.A., Abbasi Sharifabadi, A., 2017, MHD forced convection and entropy generation of CuO-water nanofluid in a microchannel considering slip velocity and temperature jump, Journal of the Brazilian Society of Mechanical Sciences and Engineering, 39, pp. 775- 790.
11. Ababaei, A., Abbaszadeh, M., Arefmanesh, A., Chamkha, A.J., 2018, Numerical simulation of double-diffusive mixed convection and entropy generation in a lid-driven trapezoidal enclosure with a heat source, Numerical Heat Transfer, Part A: Applications, 73(10), pp. 702-720.
12. Khanafer, K., Vafai, K., 2019, Applications of nanofluids in porous medium: a critical review, Journal of Thermal Analysis and Calorimetry, 135, pp. 1479-1492.
13. Hashim, I., Alsabery, A.I., Sheremet, M.A. and Chamkha, A.J., 2019, Numerical investigation of natural convection of Al2O3-water nanofluid in a wavy cavity with conductive inner block using Buongiorno's two- phase model, Advanced Powder Technology, 30(2), pp. 399-414.
14. Oztop, H. F., Abu-Nada, E., 2008, Numerical study of natural convection in partially heated rectangular enclosures filled with nanofluids, International journal of heat and fluid flow, 29(5), pp. 1326-1336.
15. Chamkha, A.J., Mansour, M.A., Rashad, A.M., Kargarsharifabad, H., Armaghani, T., 2020, Magnetohydrodynamic mixed convection and entropy analysis of nanofluid in gamma-shaped porous cavity, Journal of Thermophysics and Heat Transfer, 34(4), pp. 836-847.
16. Arefmanesh, A., Aghaei, A., Ehteram, H., 2016, Mixed convection heat transfer in a CuO–water filled trapezoidal enclosure, effects of various constant and variable properties of the nanofluid, Applied Mathematical Modelling, 40(2), pp. 815-831.
17. Aghaei, A., Sheikhzadeh, G.A., Ehteram, H.R., Hajiahmadi, M., 2015, MHD natural convection and entropy generation of variable properties nanofluid in a triangular enclosure, Challenges in Nano and Micro Scale Science and Technology, 3(1), pp. 37-45.
18. Junemoo, K., Kleinstreuer, C., 2004, A new thermal conductivity model for nanofluids, Journal of Nanoparticle research, 6, pp. 577-588.
19. Pil Jang, S., Choi, S.U., 2007, Effects of various parameters on nanofluid thermal conductivity, pp. 617-623
20. Buongiorno, J. (2006). Convective transport in nanofluids, pp. 240-250.
21. Mahmoodi, M., Sebdani, S.M., 2012, Natural convection in a square cavity containing a nanofluid and an adiabatic square block at the center, Superlattices and Microstructures, 52(2), pp. 261-275.